



# CHEMISTRY

## A European Journal



### Accepted Article

**Title:** Metal-Organic Frameworks as Hosts for Fluorinated Azobenzenes: A Path Towards Quantitative Photoswitching with Visible Light

**Authors:** Daniela Hermann, Heidi A. Schwartz, Melanie Werker, Dominik Schaniel, and Uwe Ruschewitz

This manuscript has been accepted after peer review and appears as an Accepted Article online prior to editing, proofing, and formal publication of the final Version of Record (VoR). This work is currently citable by using the Digital Object Identifier (DOI) given below. The VoR will be published online in Early View as soon as possible and may be different to this Accepted Article as a result of editing. Readers should obtain the VoR from the journal website shown below when it is published to ensure accuracy of information. The authors are responsible for the content of this Accepted Article.

**To be cited as:** *Chem. Eur. J.* 10.1002/chem.201805391

**Link to VoR:** <http://dx.doi.org/10.1002/chem.201805391>

Supported by  
**ACES**

WILEY-VCH

# Metal-Organic Frameworks as Hosts for Fluorinated Azobenzenes: A Path Towards Quantitative Photoswitching with Visible Light

Daniela Hermann,<sup>[a]</sup> Heidi A. Schwartz,<sup>[a]</sup> Melanie Werker,<sup>[a]</sup> Dominik Schaniel,<sup>[b]</sup> Uwe Ruschewitz\*<sup>[a]</sup>

Dedicated to Prof. Dr. Thomas F. Fässler on the Occasion of his 60th Birthday

**Abstract:** Fifteen new photochromic hybrid materials were synthesized by gas phase loading of fluorinated azobenzenes, namely *ortho*-tetrafluoroazobenzene (*tF*-AZB), 4H,4H'-octafluoroazobenzene (*oF*-AZB), and perfluoroazobenzene (*pF*-AZB), into the pores of the well-known metal-organic frameworks MOF-5, MIL-53(Al), MIL-53(Ga), MIL-68(Ga), and MIL-68(In). Their composition was analysed by elemental (CHNS) and DSC/TGA analysis. For *pF*-AZB<sub>0.34</sub>@MIL-53(Al) a structural model based on high-resolution synchrotron powder diffraction data was developed and the host-guest and guest-guest interactions were elucidated from this model. These interactions of O-H $\cdots$ F and  $\pi\cdots\pi$  type were confirmed by significant shifts of the O-H frequencies in loaded and unloaded MOFs of the MIL-53 and MIL-68 series. Most remarkably, all of the synthesized *F*-AZB@MOF systems can be switched with visible light and some of them show almost quantitative (> 95 %) photo-isomerization between its *E* and *Z* forms with no significant fatigue after repeated switching cycles.

## Introduction

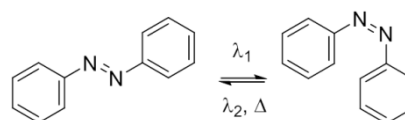
Photochromic materials have found wide-spread applications e.g. in colour changing sunglasses<sup>[1]</sup> or as data storage devices.<sup>[2]</sup> According to *Hirshberg* photochromism is the reversible structural transformation of a molecular entity between two configurations induced by irradiation with electromagnetic waves leading to a change of the resulting absorption properties.<sup>[3]</sup> These structural changes are for example *E/Z* isomerisations (e.g. azobenzenes, stilbenes) or ring-opening/-closing reactions (e.g. spiropyrans, diarylethenes).<sup>[1]</sup> For all of them the structural transformation typically leads to significant changes of the size, shape and properties like dipole moments of these molecules so that their photochromic behaviour is largely influenced by the surrounding medium. Thus the photoswitching behaviour is well established in solution,<sup>[4-8]</sup> but mainly suppressed in crystalline solids of the respective molecules due to spatial hindrance.

Accordingly, for potential applications the photochromic molecular entities are incorporated in polymers<sup>[9-11]</sup>, crystalline<sup>[12]</sup> and amorphous thin films<sup>[13-15]</sup>, porous matrices like zeolites<sup>[16-18]</sup>, or molecular cages.<sup>[19-20]</sup>

Recently, metal-organic frameworks (MOFs) were established as a new class of host materials for photochromic guests.<sup>[21-23]</sup> MOFs are hybrid materials consisting of inorganic knots, chains or layers (mainly metal-oxo units), which are bridged by rigid multifunctional organic molecules or anions (named "linker") to form crystalline porous materials with a very high structural flexibility.<sup>[24,25]</sup> To incorporate the photochromic functionality into these MOFs three general approaches were described:

- 1) The photochromic entity is part of the linker backbone of the respective MOF.<sup>[26-27]</sup> But it is a severe drawback of this approach that the large structural changes upon irradiation often lead to a degradation of the framework.
- 2) The photochromic functionality is added as a substituent to the linker.<sup>[28-37]</sup> This leads to the necessary sterical freedom for successful photoisomerisation, but like for 1) typically elaborate synthetic efforts are needed to obtain these linker molecules.
- 3) The most simple way is to directly embed the photochromic molecules into the empty pores of a MOF by gas phase loading or by solution based processes.<sup>[38]</sup> Not only the low synthetic efforts, but also the high flexibility with respect to the embedded guests are advantages of this approach.

In the following we will focus on approach 3), which has successfully been used to embed azobenzene dyes,<sup>[39,40]</sup> spiropyrans/merocyanines<sup>[41,42]</sup> and diarylethenes<sup>[43-45]</sup> in different MOF hosts. For all of them successful photoswitching of the embedded guests was proven.



**Scheme 1.** *E/Z* isomerization of azobenzene (AZB).

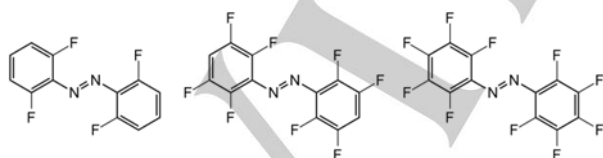
The *E/Z* isomerisation of azobenzene (abbreviated to AZB in the following), which is shown in Scheme 1, can be regarded as the prototype of photochromism. The successful embedment of AZB into the MOFs MOF-5,<sup>[40]</sup> MIL-68(In),<sup>[40]</sup> MIL-68(Ga),<sup>[40]</sup> MIL-53(Al),<sup>[40]</sup> and DMOF-1<sup>[39]</sup> was already shown, and for the latter the remote-controlled uptake and release of CO<sub>2</sub> was proven.<sup>[39]</sup> It is however a severe drawback of AZB that UV light that might

[a] Dr. D. Hermann, Dr. H. A. Schwartz, M. Werker, Prof. Dr. U. Ruschewitz  
Department of Chemistry  
University of Cologne  
GreinstraÙe 6, D-50939 Köln, Germany  
E-mail: uwe.ruschewitz@uni-koeln.de

[b] Prof. Dr. D. Schaniel  
CNRS, CRM<sup>2</sup>  
Université de Lorraine  
F-54506 Nancy, France

Supporting information for this article is given via a link at the end of the document.

interfere with the host matrix, is needed to induce the *E/Z* isomerisation. Even more, the overlapping absorption bands of the *E* and *Z* isomers result in photostationary states, i.e. a complete photoswitching of pristine AZB from *E* to *Z* and vice versa is not possible in most cases. For example, in zeolite NaY > 90 % *Z*-AZB were achieved, but here the formation of a Na<sup>+</sup>-AZB complex was postulated.<sup>[46]</sup> For AZB<sub>0.66</sub>@MIL-68(In) we only reached a maximum of ca. 30 % of the excited *Z* state under illumination with UV light ( $\lambda = 325$  nm),<sup>[40]</sup> whereas Yanai et al. found 38 % of the *Z* isomer in AZB@DMOF-1 after UV light irradiation using an ultrahigh-pressure Hg lamp.<sup>[39]</sup> However, it was shown that modifying AZB with suitable substituents will separate the absorption bands of the *E* and *Z* isomers to overcome these limitations.<sup>[47]</sup> A very elegant way is the introduction of fluorine atoms in the phenyl rings of AZB. For *ortho*-tetrafluoroazobenzene (*tF*-AZB) photostationary states with 91 % *Z* and 86 % *E* states were reached in acetonitrile solutions.<sup>[48]</sup> Furthermore, wavelengths of the visible region of the electromagnetic spectrum can be used to trigger the photoisomerization so that no longer UV light has to be applied.<sup>[48]</sup> It was successfully shown that incorporating *tF*-AZO side groups attached to suitable linker molecules into MOF structures leads to solid materials with almost quantitative *E/Z* isomerization, which can be switched with green and violet light, respectively.<sup>[35,36]</sup> In the following we will show that also by direct embedment of fluorinated derivatives of AZB in different MOF hosts following approach 3) (s. above) photochromic guest@MOF systems with an almost quantitative *E/Z* photoswitching with visible light can be obtained, even though the photoswitching unit is not covalently attached to the MOF scaffold. Furthermore, we examined the underlying host-guest interactions occurring in these guest@MOF systems and show how they influence the photoswitching properties of these composite materials. The fluorinated AZB derivatives used in this work are given in Scheme 2. Some of their optical properties are summarized in Table 1. The superior photoswitching properties of *tF*-AZB are obvious from this compilation. The crystal structures of *E*- and *Z*-*tF*-AZB were reported quite recently and compared with those of the other azobenzenes depicted in Scheme 1 and 2.<sup>[49]</sup> For thin (SURMOF) films of type HKUST-1 the successful incorporation of *tF*-AZB was already proven.<sup>[50]</sup>



**Scheme 2.** *E* isomers of *ortho*-tetrafluoroazobenzene (*tF*-AZB), 4*H*,4*H'*-octafluoroazobenzene (*oF*-AZB), and perfluoroazobenzene (*pF*-AZB) (f.l.t.r.).

<Table 1>

## Results and Discussion

### Synthesis, Composition & Stability

A few years ago we started to establish MOFs as suitable hosts for the embedment of photochromic guests like azobenzenes<sup>[40]</sup> and spiropyrans<sup>[42]</sup>. To embed the photochromic guests we developed a gas phase procedure (see Experimental Section).<sup>[40,42]</sup> Gas phase loading and loading of the molten guest<sup>[39,43]</sup> are preferable to solution based processes, as with the former any solvents can be excluded from all further considerations. Using this gas phase approach we obtained highly crystalline materials, which were accessible to characterisation by XRPD (X-ray powder diffraction) methods. In Figure 1 the XRPD patterns of activated MIL-68(Ga) and MIL-68(Ga) loaded with different photochromic azobenzene guests (pristine azobenzene, *tF*-AZB, *oF*-AZB, *pF*-AZB) are shown. As the  $2\theta$  values of the reflections are mainly unchanged after loading, it can be concluded that the MOF framework is still intact. But as the reflection intensities are drastically modulated depending on the scattering power of the embedded guest, i.e. with increasing fluorine substitution, XRPD can be used as a simple and fast method to confirm the successful embedment of the guest. Note: the intensity loss of the first reflection just below  $2\theta = 5^\circ$  upon loading with *oF*-AZB and *pF*-AZB does not indicate a decreasing crystallinity along the respective crystallographic direction, as other reflections with these indices are not affected in the same way (e.g. reflection just below  $2\theta = 20^\circ$ ). If the guest is not completely embedded in the MOF, additional reflections of the guest are visible in the respective XRPD patterns (not shown). These residues of the guest can be removed by further heating in vacuum. Even more, for spiropyran, which was attempted to be embedded in MIL-53(Al), we showed that unchanged intensities after potential gas phase loading are a clear indicator that (almost) no embedment of the guest within the pores of the MOF has taken place.<sup>[42]</sup> In Figure S21 (Supporting Information) XRPD patterns of MOF-5 loaded with different starting ratios of pristine azobenzene are shown. These patterns show that a rough estimate of the quantitative amount of the embedded guest can be obtained from these patterns and vice versa that the amount of the embedded guests molecules can be controlled by the ratio guest:host in the starting mixture.

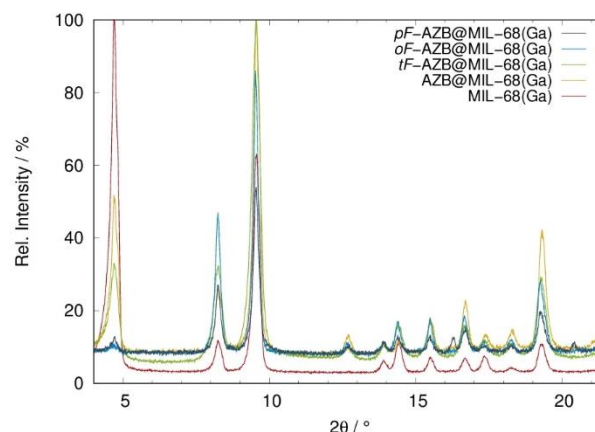


**Figure 1.** Sections of the XRPD patterns of activated MIL-68(Ga)*ht* (red), AZB@MIL-68(Ga) (yellow), *tF*-AZB@MIL-68(Ga) (green), *oF*-AZB@MIL-

68(Ga) (turquoise), and *pF*-AZB@MIL-68(Ga) (gray) (STOE Stadi P; capillaries,  $\text{CuK}\alpha_1$  radiation).

Compared with attempts to incorporate the photoactive functionality as a part of the backbone or a substituent of the linker used to construct the respective MOF the approach to embed the photochromic molecule as a guest in the MOF framework has the advantage of an easy synthetic accessibility as well as a very high versatility with respect to the MOF and the guest. One might object that the guest molecules are only weakly bonded to the MOF framework so that the thermal stability of the resulting guest@MOF systems is not high, but for azobenzene embedded in thin films of type HKUST-1 it was shown that when stored at room temperature the guest leaves the MOF very slowly with a depletion (or desorption) time constant  $\tau \approx 360$  days.<sup>[50]</sup> However, when stored at 60 °C  $\tau$  decreases significantly to 14.5 days.<sup>[50]</sup> For two *pF*-AZB containing systems of this investigation the resulting DSC/TGA curves are shown in Figure 2 and Figure S22 (Supporting Information). They show that *pF*-AZB is released from MIL-53(Al) above 150 °C (Figure 2), whereas from MOF-5 the release already starts at 100 °C (Figure S22). So the influence of the respective MOF host on the thermal stability of the resulting guest@MOF system is obvious. Nonetheless, both systems are stable at room temperature and the loss of *pF*-AZB at this temperature can be neglected. From the TGA curve of *pF*-AZB<sub>0.34</sub>@MIL-53(Al)<sup>1</sup> (Figure 2) a mass loss of 34.6 % is obtained leading to the composition *pF*-AZB<sub>0.30</sub>@MIL-53(Al), which is in very good agreement with the results of the Rietveld refinement and the elemental analysis (Table S4, Supporting Information). The smooth DSC curve confirms that neither a decomposition of the guest or the host occurs up to 500 °C. The decomposition of the MOF starts above 500 °C (not shown), which is in good agreement with its decomposition temperature given in the literature ( $T_{\text{dec.}} = 500$  °C).<sup>[53]</sup> A small peak in the TGA curve at ca. 250 °C (Figure 2) is an artefact of the balance in this measurement.

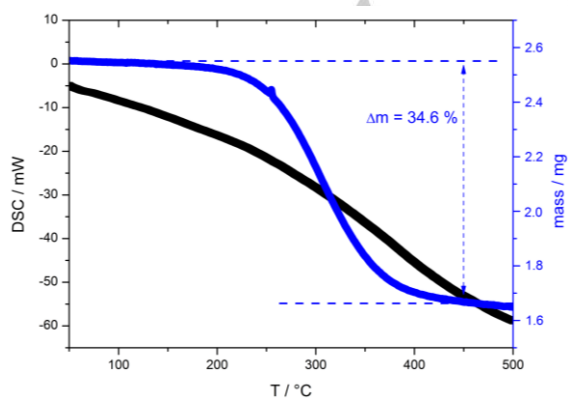


Figure 2. DSC/TGA curve of *pF*-AZB<sub>0.34</sub>@MIL-53(Al).

<sup>1</sup> Here, the composition as derived from the Rietveld refinement (see next section) is used to name this compound.

Similar results were obtained for *pF*-AZB embedded in MOF-5 (Figure S22, Supporting Information). The mass loss of 61.5 % leads to the composition *pF*-AZB<sub>3.40</sub>@MOF-5, which is again in very good agreement with the results of the elemental analysis: *pF*-AZB<sub>3.57</sub>@MOF-5 (Table S4, Supporting Information). Here, the decomposition of the MOF framework already starts at 400 °C, as described for MOF-5 in the literature.<sup>[54]</sup>

### Crystal Structure & Host-Guest Interactions

To clarify the arrangement of the fluorinated azobenzene guest embedded in a MOF host and to understand the underlying host-guest interactions as well as to confirm the reliability of the compositions obtained from elemental and DSC/TGA analysis we performed a comprehensive structural analysis with a subsequent Rietveld refinement on a selected compound. For this analysis we have chosen *pF*-AZB embedded in MIL-53(Al) for the following reasons: according to Table 3 the initial state of *pF*-AZB consists to 100 % of the *E* isomer, so that in the refinements only this isomer has to be taken into account. Furthermore, the host MIL-53(Al) shows orthorhombic symmetry, which minimizes possible disorder compared to a MOF with a higher, i.e. cubic symmetry like MOF-5. It is remarkable that compared to already published AZB<sub>0.50</sub>@MIL-53(Al) (*Pnma*, no. 62)<sup>[40]</sup> we found a symmetry change for *pF*-AZB<sub>x</sub>@MIL-53(Al) (*Imma*, no. 74). Details of the structure solution and refinement are given in the Experimental Section, in Figure 3 views of the resulting crystal structure are given. A space-filling representation was chosen to show that the guest molecules fit perfectly into the pores of MIL-53(Al) taking the respective van der Waals radii into account. H...F distances between the BDC<sup>2-</sup> linkers of the MOF and *pF*-AZB guests start at 295 pm. This value is as expected larger than the sum of the van der Waals radii of H and F (256 pm).<sup>[55]</sup> The occupancy factor of the position of the *pF*-AZB molecule refined to 8.6 % resulting in the composition *pF*-AZB<sub>0.34</sub>@MIL-53(Al). This composition, which will be used in the following to name this compound, is in reasonable agreement with the results of the elemental (*pF*-AZB<sub>0.27</sub>@MIL-53(Al)) and DSC/TGA analysis (*pF*-AZB<sub>0.30</sub>@MIL-53(Al), Figure 2 and Table S4, Supporting Information).

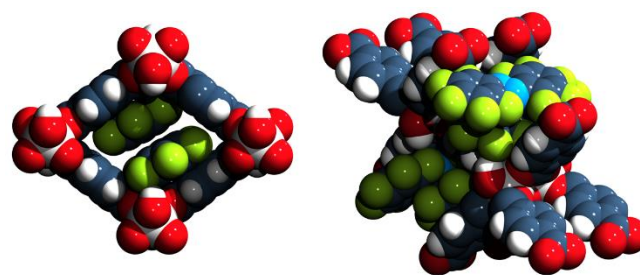
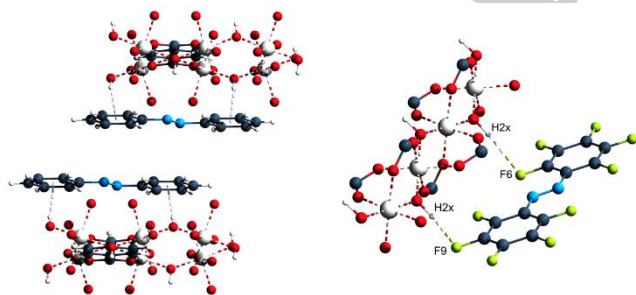


Figure 3. Space-filling presentation of the crystal structure of *pF*-AZB<sub>0.34</sub>@MIL-53(Al) with a view along a channel ([100] direction, left) and a side-view with an "opened" channel (right); Al: large white, C: grey, O: red, H: small white, F: green, N: blue spheres.

In our former work on pristine azobenzene (AZB) embedded in different MOFs we presented the crystal structures of  $AZB_{0.50}@MIL-53(Al)$  and  $AZB_{0.66}@MIL-68(Ga)$ .<sup>[40]</sup> As in all these investigations (Rietveld, elemental and DSC/TGA analysis) a good agreement for the amount of the embedded guest molecules was found, we conclude that all methods are suitable to quantify the loading. In Figure 4 the dominating host-guest interactions in  $AZB_{0.50}@MIL-53(Al)$ <sup>[40]</sup> and  $pF-AZB_{0.34}@MIL-53(Al)$  are compared, as assigned after close inspection of both crystal structures. In  $AZB_{0.50}@MIL-53(Al)$  O-H $\cdots\pi$  interactions between the hydroxyl group of the MOF and both phenyl rings of AZB (O-H $\cdots$ C = 265 and 276 pm) are found. These interactions are depicted in Figure 4 (left) as dashed lines. Furthermore a parallel orientation of the phenyl rings of the BDC<sup>2-</sup> linkers and the AZB guests suggests  $\pi\cdots\pi$  interactions. The planes of two AZB guests are separated by 349 pm and the planes of a guest and a BDC<sup>2-</sup> linker by 382 pm. So for the latter only weak interactions must be assumed. In both cases the centres of the rings are shifted by approx. 300 pm pointing to a parallel displaced stacking (offset stacked). Some host-guest interactions found in  $pF-AZB_{0.34}@MIL-53(Al)$  are depicted in Figure 4 (right). Contrary to  $AZB_{0.5}@MIL-53(Al)$  O-H $\cdots F$  interactions (shortest O-H $\cdots F$  distance: 213 pm) seem to dominate and only weak O-H $\cdots\pi$  interactions are observed (shortest O-H $\cdots C$  distance: 281 pm compared to 265 pm in  $AZB_{0.50}@MIL-53(Al)$ ). But this finding is not surprising, as the high degree of fluorination of the  $pF-AZB$  guest leads to an inversion of its quadrupole moment, i.e. the fluorine substituents bear the negative charge and the aromatic ring can no longer act as an electron donor.<sup>[56]</sup> The orientation of the phenyl rings of two guest molecules is not in agreement with attractive  $\pi\cdots\pi$  interactions. 320 pm is found as the shortest C-C distance between a  $pF-AZB$  guest and the BDC<sup>2-</sup> linker. The rings are arranged almost directly one above each other with only a very small shift, which is in-between a stacked and an offset stacked arrangement.<sup>[57]</sup> This can also be explained by the inverted quadrupole moment of the perfluorinated ring leading to an interaction with the unfluorinated phenyl ring of the BDC<sup>2-</sup> linker of a different type. These interactions result in a slight shift of the frequency of  $\tilde{\nu}(C=C)$  from 1506 cm<sup>-1</sup> in the IR spectrum of unloaded MIL-53(Al) to 1513 cm<sup>-1</sup> in the IR spectrum of  $pF-AZB_{0.34}@MIL-53(Al)$ .



**Figure 4.** Details of the crystal structures of  $AZB_{0.5}@MIL-53(Al)$ <sup>[40]</sup> (left) and  $pF-AZB_{0.34}@MIL-53(Al)$ <sup>[this work]</sup> (right) emphasizing some of the occurring host-guest interactions; colour coding as in Figure 3.

To analyse these host-guest and guest-guest interactions in more detail IR spectra of the activated ("empty") and loaded MOF were recorded. Especially the MOFs of type MIL-53 and MIL-68 are well-suited for such investigations, as the OH groups in these MOFs are sensitive probes for such interactions. All samples were prepared under inert conditions (glovebox) and the spectrometer itself was also housed in a glovebox to provide completely inert conditions and to exclude any water impurities. In Table 2 the shifts of the resulting O-H frequencies are summarized as  $\Delta\tilde{\nu}$  values, i.e. referenced to  $\tilde{\nu}(OH)$  of the activated ("empty") MOF.

**Table 2.** Shifts of IR frequencies of O-H stretching vibrations in loaded MOFs of the MIL-53 and MIL-68 series referenced to the activated MOF.

	<i>E</i> isomer $\Delta\tilde{\nu} / \text{cm}^{-1}$	<i>Z</i> isomer $\Delta\tilde{\nu} / \text{cm}^{-1}$
$AZB_{0.50}@MIL-53(Al)$	-39	-39
<i>tF-AZB</i> <sub>0.19</sub> @MIL-53(Al)	-11 / -17 <sup>[a]</sup>	-28
<i>pF-AZB</i> <sub>0.34</sub> @MIL-53(Al)	-10	-10
$AZB_{0.66}@MIL-68(Ga)$	-39	-39
<i>tF-AZB</i> <sub>0.58</sub> @MIL-68(Ga)	-14	-24
<i>pF-AZB</i> <sub>0.63</sub> @MIL-68(Ga)	-3 / -10 <sup>[a]</sup>	-3 / -10 <sup>[a]</sup>
$AZB_{0.66}@MIL-68(In)$	-55	-55
<i>tF-AZB</i> <sub>0.57</sub> @MIL-68(In)	-49	-12
<i>pF-AZB</i> <sub>0.32</sub> @MIL-68(In)	-16	-16

[a] split signals

The most significant shifts were obtained for AZB as guest. This points to the fact that the O-H $\cdots\pi$  and  $\pi\cdots\pi$  interactions discussed for  $AZB_{0.50}@MIL-53(Al)$  are obviously stronger than the O-H $\cdots F$  and  $\pi\cdots\pi$  interactions found in  $pF-AZB_{0.34}@MIL-53(Al)$ . The guest-guest and host-guest interactions with *tF-AZB* seem to be somewhere in-between: in MIL-68(In) a strong shift was found, whereas smaller shifts are observed for *tF-AZB* embedded in MIL-53(Al) and MIL-68(Ga). Possibly, *tF-AZB* is able to form different types of interactions (O-H $\cdots F$ , C-H $\cdots\pi$  etc.), which are dependent on the specific arrangement of the guest within the MOF pores. This is supported by the significant shifts upon *E*  $\rightarrow$  *Z* isomerization, which are specific for *tF-AZB* as guest. This will be discussed in more detail in the next chapter, where also a correlation between the photochromic properties and the host-guest and guest-guest interactions, as indicated by the results documented in Table 2, will be attempted.

### Photochromic Properties

In our previous work we showed that IR spectroscopy is well-suited to characterize the photochromic behaviour of azobenzene<sup>[40]</sup> and spiropyran<sup>[42]</sup> embedded in different MOF hosts, as the IR bands of the guest hardly overlap with those of the MOF host (Figure 5). Therefore it allows for a direct quantitative analysis of the switching process via the determination of the changes of the relevant IR bands. This procedure seems to be preferable to the elution of the guest and analysis of the *E/Z* ratio by e.g. ultraperformance liquid chromatography (UPLC).<sup>[52]</sup>

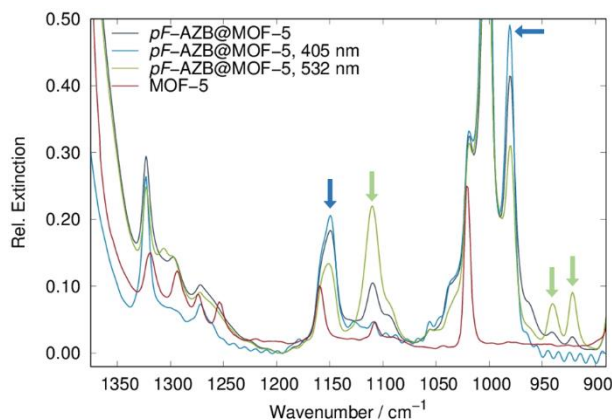


**Figure 5.** IR spectra of *pF*-AZB@MOF-5 after light induced isomerization with  $\lambda = 532$  nm ( $E \rightarrow Z$ ) and  $\lambda = 405$  nm ( $Z \rightarrow E$ ). The IR spectra of the as-synthesized state and pristine MOF-5 are given as a dark grey and a red curve, respectively. Arrows mark bands assigned to the *E* (blue) and *Z* (green) isomer.

We therefore used this approach to characterize the photochromic behaviour of the novel guest@MOF systems. In Figure 5-7 and Figures S23-S25 (Supporting Information) the IR spectra, we obtained before and after illumination with light of different wavelengths, are given for *pF*-AZB@MOF-5, *tF*-AZB@MIL-68(In), and *pF*-AZB@MIL-68(In). After testing several wavelengths for photoswitching we observed that the best results were obtained with  $\lambda = 532$  nm for  $E \rightarrow Z$  and  $\lambda = 405$  nm for  $Z \rightarrow E$  switching. In Table 3 the results of the quantitative analyses of the IR spectra are summarized. For each of the investigated systems the maximum amounts of *E* and *Z* isomers are given, which were obtained by the illumination experiments. Additionally, the composition of the initial state (before illumination) is listed. More details are given in the Experimental Section.

*E-pF*-AZB shows absorption maxima at  $\lambda = 310$  nm and  $\lambda = 453$  nm in solution.<sup>[52]</sup> We have chosen *pF*-AZB<sub>3,57</sub>@MOF-5 for first illumination experiments with different wavelengths. The changes in the obtained IR spectra (Figure 5) after irradiation were compared with the spectra given in the literature and specific bands were assigned to the two isomers. For *pF*-AZB<sub>3,57</sub>@MOF-5 the highest amount of *Z-pF*-AZB was obtained by illumination with green light ( $\lambda = 532$  nm) in good agreement with the results obtained for solutions (cp. Table 1).<sup>[52]</sup> The back transformation  $Z \rightarrow E$  was achieved by illumination with violet light ( $\lambda = 405$  nm). Similarly, the isomerization of *tF*-AZB in solution was described with  $\lambda > 450$  nm ( $E \rightarrow Z$ , 91 %) and  $\lambda = 410$  nm ( $Z \rightarrow E$ , 86 %).<sup>[48,52]</sup> For *tF*-AZB embedded in MIL-68(In) (Figure 6) we achieved the highest amount of  $E \rightarrow Z$  isomerization with  $\lambda = 532$  nm and  $Z \rightarrow E$  isomerization with  $\lambda = 405$  nm, similar to *pF*-AZB. We also used  $\lambda = 476$  nm to trigger the  $E \rightarrow Z$  isomerization in *tF*-AZB@MIL-68(In). As can be seen in Figure 6 an  $E \rightarrow Z$  isomerization was achieved, but the amount of the *Z* isomer was significantly smaller than the amount obtained with  $\lambda = 532$  nm. With all other MOF hosts or with *oF*-AZB as third photochromic guest used in this investigation the best results

(maximum of the respective photo isomer) were obtained by irradiation with  $\lambda = 532$  nm ( $E \rightarrow Z$ ) and  $\lambda = 405$  nm ( $Z \rightarrow E$ ). Notably, fluorination of azobenzene allows photoswitching with visible light similar to solutions,<sup>[48,52]</sup> whereas for pristine azobenzene UV light ( $\lambda = 325$  nm) has to be used for the  $E \rightarrow Z$  isomerization.<sup>[40]</sup>

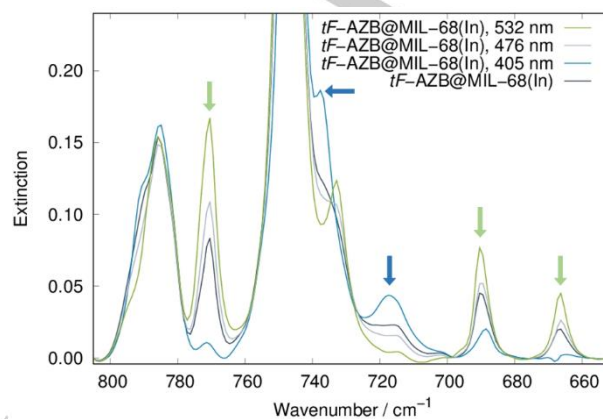


**Figure 6.** IR spectra of *tF*-AZB@MIL-68(In) after light induced isomerization with  $\lambda = 476$  nm / 532 nm ( $E \rightarrow Z$ ) and  $\lambda = 405$  nm ( $Z \rightarrow E$ ). The as-synthesized state is given as a dark grey curve. Arrows mark bands assigned to the *E* (blue) and *Z* (green) isomer.

Remarkably, in some spectra the bands of one isomer are almost completely extinguished after irradiation. In *pF*-AZB@MIL-68(In) (Figure 7) the band at  $1110$   $\text{cm}^{-1}$ , assigned to *Z-pF*-AZB, is no longer observed after irradiation with violet light ( $\lambda = 405$  nm), i.e. the *Z* isomer is completely transformed to the respective *E* isomer by irradiation. Similarly, the intensity of the band at approx.  $770$   $\text{cm}^{-1}$  in *tF*-AZB@MIL-68(In) (Figure 6) decreases strongly upon irradiation with violet light, again pointing to an almost complete  $Z \rightarrow E$  isomerization. Upon irradiation with green light ( $\lambda = 532$  nm) the intensities of these bands increase indicating a successful  $E \rightarrow Z$  isomerization.

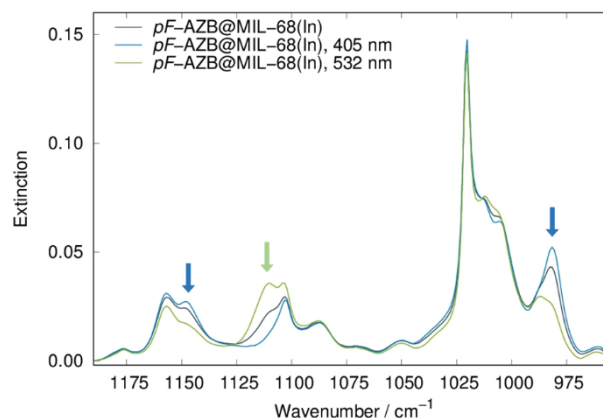


**Figure 7.** IR spectra of *pF*-AZB@MIL-68(In) after light induced isomerization with  $\lambda = 532$  nm ( $E \rightarrow Z$ ) and  $\lambda = 405$  nm ( $Z \rightarrow E$ ). The as-synthesized state is

given as a dark grey curve. Arrows mark bands assigned to the *E* (blue) and *Z* (green) isomer.

As a control experiment pure crystalline *tF*-AZB and *pF*-AZB were investigated under the same conditions. The initial state (before illumination) of *pF*-AZB consists of a mixture of both isomers and photochemical conversion of one isomer into the other was not possible in the crystalline material. In contrast, *tF*-AZB shows photo-isomerization in the solid state as well (Figure S23a), Supporting Information). By illumination of the initial state containing also a mixture of both isomers with violet light ( $\lambda = 405$  nm) a complete isomerization to 100 % *E*-*tF*-AZB was achieved. Illumination with green light ( $\lambda = 532$  nm) led to 37 % of the *Z* isomer.

<Table 3>

As described in our former work for AZB embedded in different MOF hosts only a maximum of 30 % *Z*-AZB was reached upon irradiation.<sup>[40]</sup> For potential applications this is certainly a drawback as well as the necessity of UV light to induce the photo-isomerization. As highlighted in Table 3 the situation is different for fluorinated azobenzenes as photochromic guests. All compounds with *pF*-AZB as guest molecule can be transferred to 100 % of the *E* isomer by illumination with violet light ( $\lambda = 405$  nm). However, with green light only a maximum of 79 % *Z* isomer is reached within a MIL-68(In) host. For potential applications, hybrid materials with embedded *tF*-AZB are preferable, as in almost all MOF hosts *E* and *Z* ratios above 90 % were reached (Table 3). One might speculate that the size of the MOF pores influences the photo-isomerization, as for *pF*-AZB as photochromic guest the largest *Z* ratio is observed within the large pores of MIL-68(In). However, within the pores of MOF-5 with a similar size only 50 % of *Z*-*pF*-AZB were reached and no such size-dependence is observed for different MOFs with *tF*-AZB as guest at all. In Table 2 the shifts of OH frequencies of the MIL-53/MIL-68 frameworks upon guest loading are given. It is quite remarkable that upon irradiation and photo-isomerization these signals show the most significant shifts for systems with *tF*-AZB guests. Two exemplary IR spectra are given in Figure 8. Upon irradiation and photo-isomerization the host-guest and guest-guest interactions change in these *tF*-AZB@MOF systems. Consequently, the ratio of *E* and *Z* isomers seems to be less influenced by the pore size of the respective MOF host, but more significantly by the underlying host-guest and guest-guest interactions, which were discussed above for  $\text{AZB}_{0.50}$ @MIL-53(Al) and  $\text{pF-AZB}_{0.34}$ @MIL-53(Al) (Figure 4). For a rational design of an optimized guest@MOF system it seems to be indispensable to understand these interactions in more detail.

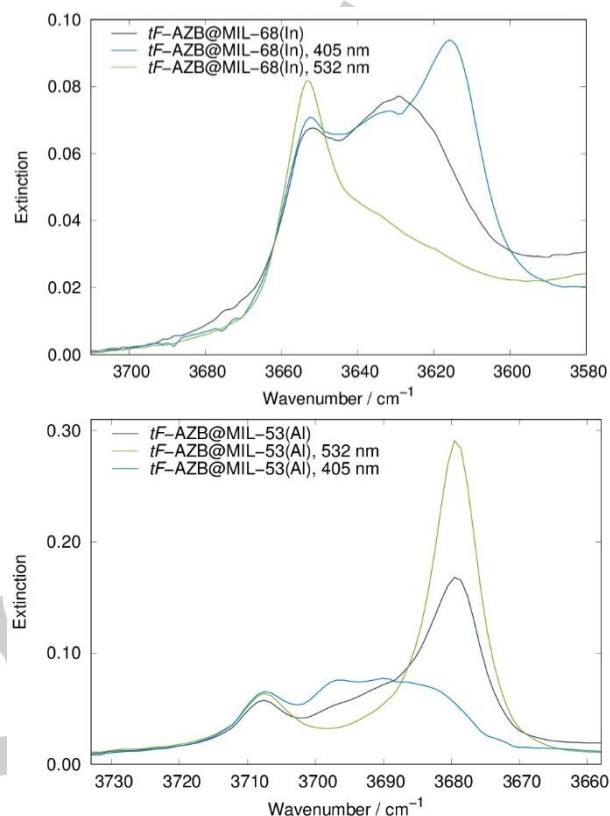


**Figure 8.** Sections (region of OH frequencies) of the IR spectra of *tF*-AZB@MIL-68(In) (above) and *tF*-AZB@MIL-53(Al) (below) after light induced isomerization with  $\lambda = 532$  nm (*E*→*Z*) and  $\lambda = 405$  nm (*Z*→*E*). The as-synthesized state is given as a dark grey curve.

It was a remarkable finding of our work on AZB embedded in different MOFs that for  $\text{AZB}_{0.50}$ @MIL-53(Al) no photo-isomerization was achieved even after very long irradiation times.<sup>[40]</sup> From the crystal structure it was concluded that the AZB guests are densely packed within the pores of MIL-53(Al) so that photo-isomerization is hindered for steric reasons.<sup>[40]</sup> As can be seen in Table 3, *tF*-AZB (100 % *Z*), *oF*-AZB (56 % *Z*), and *pF*-AZB ("little *Z*") embedded in MIL-53(Al) allow photo-isomerization, at least to some extent. But from chemical analysis (Table S4, Supporting Information) it was found that the loading in these systems is different:  $\text{guest}_x$ @MIL-53(Al) with  $x = 0.50$  for AZB,  $x = 0.19$  for *tF*-AZB,  $x = 0.18$  for *oF*-AZB, and  $x = 0.30$  (or 0.34 depending on the analytical method) for *pF*-AZB. Even when considering the different volumes of the guests (AZB:  $V/Z = 248.33(5) \text{ \AA}^3$ ; *tF*-AZB:  $V/Z = 272.90(2) \text{ \AA}^3$ ; *oF*-AZB:  $V/Z = 289.90(5) \text{ \AA}^3$ ; *pF*-AZB:  $V/Z = 284.65(5) \text{ \AA}^3$ )<sup>[49]</sup> the packing of AZB ( $x = 0.50$ ) within the pores of MIL-53(Al) is much denser than that of *tF*-AZB ( $x = 0.19$ ). Hence, varying *Z* ratios for the different guest@MOF systems are not surprising. Kitagawa and co-workers embedded AZB in flexible DMOF-1 and found a reversible structural transformation of the MOF framework upon photo-isomerization of the AZB guest molecule,

which was used to remote-control the uptake and release of CO<sub>2</sub>.<sup>[39]</sup> This structural transformation was reached, although photo-isomerization only led to a *Z/E* ratio of 38:62.<sup>[39]</sup> As MIL-53(Al) and its Ga analogue are also known to show flexible (“breathing”) behaviour upon guest inclusion,<sup>[53,58]</sup> we tested our guest@MIL-53 systems for such behaviour. In Figures S26 and S27 (Supporting Information) the synchrotron powder diffraction patterns of *tF-AZB*<sub>0.19</sub>@MIL-53(Al) (capillary,  $\varnothing = 0.3$  mm) after irradiation with green ( $\lambda = 532$  nm; several hours) and violet light ( $\lambda = 405$  nm; several hours) are compared with those of non-irradiated *tF-AZB*<sub>0.19</sub>@MIL-53(Al). As the reflection positions are unchanged no structural transformation has taken place under these conditions. Slight changes of the reflection intensities indicate a different arrangement of the *tF-AZB* guests within the pores of MIL-53(Al) upon irradiation. In Figure S28 (Supporting Information) smaller sections of the synchrotron powder diffraction patterns are compared. The peaks obtained upon violet light irradiation ( $\lambda = 405$  nm, *Z*→*E* isomerization) appear slightly broadened. It should be noted that the low penetration depth of UV/vis light into solid matter might be the reason that no structural changes of *tF-AZB*<sub>0.19</sub>@MIL-53(Al) were observed upon irradiation with green or violet light. Notably, differing results were published for structural transformations of flexible MOF hosts induced by photo-isomerization of embedded guests. *Kitagawa* and co-workers reported such an effect for AZB embedded in flexible DMOF-1,<sup>[39]</sup> whereas photo-isomerization of related PAP (2-phenylazopyridine)<sup>[59]</sup> or DTE (1,2-bis(2,5-dimethyl-thien-3-yl)-perfluorocyclopentene)<sup>[43]</sup> did not lead to a structural transformation of the same host upon irradiation.

## Conclusions

In summary, we have synthesized and characterized 15 new photochromic materials by embedment of fluorinated azobenzenes, namely *ortho*-tetrafluoroazobenzene (*tF-AZB*), 4H,4H'-octafluoroazobenzene (*oF-AZB*), and perfluoroazobenzene (*pF-AZB*), into the pores of the five well-known MOFs, i.e. MOF-5, MIL-53(Al), MIL-53(Ga), MIL-68(Ga), and MIL-68(In). The successful embedment was confirmed by X-ray powder diffraction and the amount of loading determined from elemental (CHNS), DSC/TGA, and – for one example – Rietveld analysis. The latter was performed on *pF-AZB*<sub>0.34</sub>@MIL-53(Al). From the resulting crystal structure host-guest and guest-guest interactions were elucidated revealing O-H⋯F and  $\pi\cdots\pi$  type interactions, which were compared with the interactions found in the already described crystal structure of *AZB*<sub>0.5</sub>@MIL-53(Al). In compounds with MOFs of the MIL-type series shifts of the O-H frequencies of the respective hosts were used to quantitatively assign these interactions. Notably, the largest shifts and thus strongest interactions were found for unfluorinated azobenzene as guest. Similarly, Bléger and co-workers used the O-H stretching frequencies of an UiO-66 type MOF with *tF-AZB* side groups to follow the photo-isomerization in this system.<sup>[35]</sup>

However, the most remarkable finding of our investigations is that for some of the synthesized *F-AZB*@MOF systems an

almost quantitative (> 95 %) switching between *E* and *Z* isomers was observed in a solid state material. This core message of our work is summarized in Figure 9. It is also notable that this switching can be reached with green and blue light only, i.e. no UV light is needed to trigger the *E/Z* isomerisation.

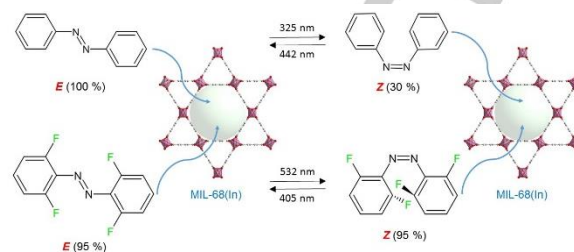


**Figure 9.** Almost quantitative *E/Z* isomerisation in *tF-AZB*@MIL-68(In) with green and blue light, respectively.

Quantitative switching in solids is still rare, but not unprecedented.<sup>[36,60]</sup> From the results of the photophysical investigations summarized in Table 3 *tF-AZB* is the most interesting guest molecule, which already showed very remarkable photochromic properties in solution (Table 1) or as a side group in other MOFs.<sup>[35,36]</sup> Concerning the host material MIL-68(In) seems to be preferable due to its higher chemical stability compared to e.g. MOF-5 and the high photo-isomerization rates that were achieved within this host (Table 3). Therefore, we have chosen *tF-AZB*<sub>0.57</sub>@MIL-68(In) to investigate the photochemical stability of this system. In Figure 10 the ratios of *E-tF-AZB* after three switching cycles with  $\lambda = 532$  nm and  $\lambda = 405$  nm, resp. are shown, which reveal no significant fatigue in these measurements. For possible applications it should be noted that a successful synthesis of thin films of MIL-68(In) has already been described.<sup>[61]</sup>

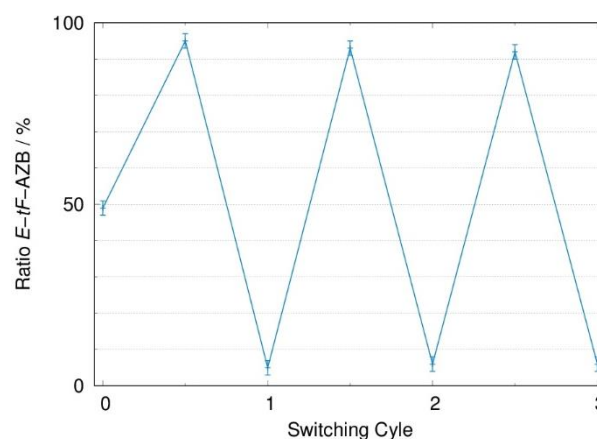


**Figure 10.** Ratio of *E-tF-AZB* in *tF-AZB*<sub>0.57</sub>@MIL-68(In) after three switching cycles and irradiation with  $\lambda = 532$  nm and  $\lambda = 405$  nm, resp.. For the standard deviation a value of  $\pm 2$  % was estimated.

To improve the photochromic properties of the presented *F*-AZB@MOF systems it is essential to understand the underlying host-guest and guest-guest interactions in more detail. In our investigation we give first insights how these interactions can be determined. It is very remarkable that for *tF*-AZB as guest the IR frequencies show the most significant shifts upon photoisomerization (Table 2). This indicates that the host-guest and guest-guest interactions change upon *E/Z* isomerization. Hence, influencing these interactions is a powerful tool to modulate the photochromic properties of these materials. Additionally, we found that the photochromic properties are affected by the size/shape of the MOF's pore, by the degree of guest loading, i.e. the packing of the guest molecules within the MOF's pores, and/or by the chemical environment given by the MOF pores. For spiropyrans embedded in MOFs we used the solvatochromic behaviour of the excited merocyanine form to investigate the influence of the MOF's polarity on the photostationary state.<sup>[42]</sup> But, as the excited *Z* form of azobenzene is not solvatochromic, this approach cannot be used here and any further interpretation remains speculative at the moment. Nonetheless, to improve the photophysical properties of these guest@MOF systems for possible applications it is indispensable to understand the underlying interactions in more detail, which is the focus of our current research in this field.

## Experimental Section

**MOF synthesis.** The colourless metal-organic frameworks MOF-5,<sup>[54]</sup> MIL-53(Al),<sup>[53]</sup> MIL-53(Ga),<sup>[58]</sup> MIL-68(Ga),<sup>[62]</sup> and MIL-68(In)<sup>[62]</sup> were selected for this investigation. Details of their syntheses are given in the Supporting Information. MOF-5 was provided by BASF and used without any further purification.

**Synthesis of fluorinated azobenzenes.** For the synthesis of *tF*-AZB and *oF*-AZB we used the protocol that was described earlier in detail.<sup>[49]</sup> *tF*-AZB: C<sub>12</sub>H<sub>6</sub>F<sub>4</sub>N<sub>2</sub> (254.19): Calcd – C, 56.70%, H, 2.38%, N, 11.02%; Found – C, 56.92%, H, 2.89%, N, 10.35%; *oF*-AZB: C<sub>12</sub>H<sub>2</sub>F<sub>8</sub>N<sub>2</sub> (326.15): Calcd – C, 44.19%, H, 0.62%, N, 8.59%; Found – C, 44.64%, H, 0.85%, N, 7.96%.

***pF*-AZB** was synthesized mainly following the procedures given in the literature.<sup>[63,64]</sup> 0.5 g pentafluoroaniline (2.73 mmol) were dissolved in 30 mL toluene and 3.03 g Lead(IV)-acetate (6.83 mmol) were added, whereon the suspension turned red. After stirring at room temperature overnight the brown precipitate was filtered off. The solution was washed with acetic acid (50%) and the organic phase was dried with MgSO<sub>4</sub>. After removing the solvent at reduced pressure the residue was purified by column chromatography (CH<sub>2</sub>Cl<sub>2</sub>:*cyclo*-hexane = 3:7). 128.8 mg (yield: 37%) perfluoroazobenzene were obtained as a red solid. NMR signals were assigned according to the literature:<sup>[64]</sup> <sup>19</sup>F-NMR (282MHz, CDCl<sub>3</sub>): δ /ppm = -161.2 (m, 4F, trans-2F, 2'F, 6F, 6'F), -158,6 (m, 4F, cis-2F, 2'F, 6F, 6'F), -150,4 (m, 2F, cis-4F, 4'F), -148,3 (m, 6F, trans-F3, F3', F4, F4', F5, F5'), -146,6 (m, 4F, cis-F3, F3', F5, F5'). C<sub>12</sub>F<sub>10</sub>N<sub>2</sub> (362.13): Calcd – C, 39.80%, H, 0%, N, 7.74%; Found – C, 39.65%, H, 0.40%, N, 6.77%. Small amounts of hydrogen might result from minor amounts of moisture or solvents (CH<sub>2</sub>Cl<sub>2</sub> or *cyclo*-hexane).

**Preparation of guest@MOF systems (guest: *tF*-AZB, *oF*-AZB, *pF*-AZB).** In general a mixture of the respective activated MOF was loaded

with the azobenzene via a gas phase procedure. Under reduced pressure ( $\sim 5 \times 10^{-2}$  mbar) the respective AZB guest was sublimed on to the activated MOF, which was heated from 50 °C to 70 °C (*tF*-AZB) or 75 °C (*oF*-AZB, *pF*-AZB) for 2-3 hours. The end of the loading process was recognized, when no longer red crystals of the azobenzene are visible on the MOF material. The excess of the respective azobenzene resublimated at the top of the glass tube. To prevent the absorption of water or the decomposition of the MOF upon contact with air or moisture, all compounds were stored in a glovebox under a dry argon atmosphere (H<sub>2</sub>O < 1 ppm, O<sub>2</sub> < 1 ppm), where all further handling was carried out. In Table S1 (Supporting Information) the detailed weighted samples of all experiments are listed. A photograph of some of the resulting powders is given as Figure S5 (Supporting Information). The purity and composition of the resulting composites guest@MOF were analyzed by XRPD (Le Bail fits: Table S2, Figures S6-S19 in the Supporting Information) and elemental analysis (Table S3, Supporting Information). The resulting compositions are summarized in Table S4 (Supporting Information). Details of the methods are given below.

**X-ray Powder Diffraction.** Laboratory measurements were carried out on a STOE Stadi P diffractometer (Ge monochromator, PSD detector) with Cu K $\alpha_1$  radiation. Data were collected at 298 K between 4 and 80.59° in 2 $\theta$  with steps of 0.01° and a measurement time of 5 s/step. For each sample four such scans were added. Alternatively, data were recorded on a Huber G670 diffractometer (Ge monochromator, image plate detector, room temperature, Cu K $\alpha_1$  radiation), ca. 120-800 min per scan. Samples were sealed in glass capillaries ( $\varnothing = 0.3 - 0.5$  mm) under inert conditions (Argon filled glovebox) prior to all measurements.

**Synchrotron Powder Diffraction.** High-resolution synchrotron powder diffraction data were recorded at the Swiss Norwegian BeamLine (SNBL, BM01B)<sup>[65]</sup> at the European Synchrotron (ESRF, Grenoble/France). The wavelength was calibrated with a Si standard NIST 640c to 0.50195 Å and 0.50544 Å, respectively. The diffractometer is equipped with six counting channels, delivering six complete patterns collected with a small 1.1° offset in 2 $\theta$ . A Si(111) analyser crystal is mounted in front of each NaI scintillator/photomultiplier detector. Data were collected at 298 K and 120 K (cryostreamer) with steps of 0.002° (2 $\theta$ ) and 100-500 ms integration time per data point. Typical recording times were 20-60 min per scan. For each sample 5-8 such scans were added. Data from all detectors and scans were averaged and added to one pattern with local software.

An additional synchrotron powder diffraction pattern was collected at beamline BL9 of the DELTA synchrotron radiation facility, Dortmund.<sup>[66]</sup> The measurement was performed at 295 K with a wavelength of  $\lambda = 0.81577$  Å using a NaI scintillation detector.

For all experiments the substances were filled in glass capillaries ( $\varnothing = 0.7 - 1.0$  mm) and sealed under an argon atmosphere. The capillaries were mounted on spinning goniometers.

**Analysis of powder diffraction data.** The WinXPow software package<sup>[67]</sup> was used for raw data handling and visual inspection of the data. To determine the unit cell parameters of the resulting guest@MOF systems precisely, Le Bail fits in Jana2006<sup>[68]</sup> were performed by refining the lattice parameters, zero shift, background, and profile parameters (pseudo-Voigt) for each pattern. Depending on the instrument also parameters for reflection asymmetry and anisotropy were included in the refinements. The results of these Le Bail fits are summarized in Table S2 and the plots of these fits are shown in Figures S6-S19 (all Supporting Information). They were visualized using Gnuplot 4.6.<sup>[69]</sup>

**Structure Solution and Refinement.** The high quality diffraction pattern of  $pF\text{-AZB}_{0.34}@MIL\text{-}53(\text{Al})$  obtained at the ESRF at 120 K was used to elucidate the arrangement of the guest within the pores of this MOF. For the structure solution, the atomic positions of MIL-53(Al)-0.7H<sub>2</sub>bdc<sup>[70]</sup> were used as starting parameters of the host together with the unit cell parameters obtained from the Le Bail fits. Furthermore, the known molecular structure of *E*-perfluoroazobenzene<sup>[71]</sup> was introduced on the starting position 000 in FOX.<sup>[72]</sup> The global optimization algorithm was run in the parallel tempering mode and converged after approximately 130000 trials for  $pF\text{-AZB}@MIL\text{-}53(\text{Al})$  ( $R_p = 0.2452$  and  $wR_p = 0.1699$ ). The occupancy of  $pF\text{-AZB}$  was fixed at 0.125 in the solution process. The resulting structural model was used as a starting model for a Rietveld refinement with GSAS.<sup>[73]</sup> To get a stable refinement, the *E*-perfluoroazobenzene molecules, as well as the benzenedicarboxylate anions of the MOF, were fixed with soft constraints (bond lengths, angles, and planes according to the literature values).<sup>[70,71]</sup> The isotropic displacement parameters of the atoms of the  $pF\text{-AZB}$  guest and the host were coupled with constraints and refined afterward, if possible. In the final refinements also the occupancy of the guest was refined resulting in  $pF\text{-AZB}_{0.34}@MIL\text{-}53(\text{Al})$ . This occupancy is in good agreement with the result of the elemental analysis:  $pF\text{-AZB}_{0.3}@MIL\text{-}53(\text{Al})$  (Tables S3 and S4, Supporting Information). The final refinement of  $pF\text{-AZB}_{0.34}@MIL\text{-}53(\text{Al})$  converged slowly with a total of 119 parameters ( $R_p = 0.0858$  and  $wR_p = 0.1082$ ). The resulting fit is given as Figure S20 and selected details of the Rietveld refinement are summarized in Table S5, both Supporting Information. The reliability of the resulting structural model is corroborated by the good fit (Figure S20), the almost coincident compositions obtained from Rietveld refinement ( $x = 0.34$ ) and elemental analysis ( $x = 0.30$ ) as well as the reasonable resulting distances between the  $pF\text{-AZB}$  guest and the MOF host, which have already been discussed in the "Results and Discussion" paragraph. Diamond<sup>[74]</sup> was used for the visualization of the crystal structure of  $pF\text{-AZB}_{0.34}@MIL\text{-}53(\text{Al})$ .

**Elemental Analysis.** Elemental analysis of carbon, hydrogen, and nitrogen was performed with a HEKAtech GmbH EuroEA 3000 Analyser. In a glovebox, approximately 2 mg of each compound was filled into a tin cartridge. Theoretical values were calculated for different ratios guest:host and compared with the experimental values. The composition with the best agreement in all three values (C, H, N content) was chosen as the most likely one and used in the following (Tables S3 and S4 in the Supporting Information). Compounds with MIL-53(Ga) as host were excluded from these calculations, as weak extra reflections in the XRPD patterns of the as-synthesized MOF indicated that it was not obtained as a single-phase product.

**NMR spectroscopy.** <sup>1</sup>H and <sup>19</sup>F NMR spectra were recorded on a BRUKER Avance 300 MHz spectrometer in deuterated CDCl<sub>3</sub> solutions at room temperature (<sup>1</sup>H: 300.13 MHz; <sup>19</sup>F: 282 MHz). The spectra were analysed with the ACD/NMR Processor software.<sup>[75]</sup>

**IR spectroscopy.** IR spectra without illumination were recorded with a Bruker ALPHA FT-IR spectrometer (Platinum ATR module and diamond crystal). The spectrometer was housed in a glovebox (Argon atmosphere) to provide inert conditions. IR measurements under photo-irradiation were performed on transparent KBr pellets (dried at 60 °C; 10 t for 30 min) on a Nicolet 5700 spectrometer (250 – 4000 cm<sup>-1</sup>, resolution: 2 cm<sup>-1</sup>). During the measurements the sample chamber was evacuated to 10<sup>-5</sup> bar to enhance the quality of the spectra as well as to improve the life time of the transparent pellets. After recording the IR spectra of the as-synthesized state, the compounds were illuminated with 532 nm laser light to induce the *E*→*Z* isomerization. To investigate the reconversion to *E*-azobenzenes, the compounds were illuminated with 405 nm laser light. For *tF*-AZB also illumination with  $\lambda = 476$  nm was tested (Figure 6). The following exposure times ( $t_{exp}$ ) and radiant exposures ( $E/A$ ) were applied

for the different fluorinated AZB guests: *pF*-AZB ( $t_{exp} = 30\text{-}60$  min;  $E/A = 24\text{-}95$  J/cm<sup>2</sup>), *oF*-AZB ( $t_{exp} = 15\text{-}58$  min;  $E/A = 12\text{-}95$  J/cm<sup>2</sup>), and *tF*-AZB ( $t_{exp} = 23\text{-}126$  min;  $E/A = 23\text{-}278$  J/cm<sup>2</sup>). For *pF*-AZB ( $t_{exp} = 780$  min) and *tF*-AZB ( $t_{exp} = 840$  min) also long exposures overnight were tested.

For a quantitative analysis the extinctions of the bands of the *E* and *Z* isomers were determined (integration of the areas under the respective IR peaks after subtraction of the base line) and the maximum amount of the respective isomer was calculated based on the linear relationship between the concentration of a species and the extinction in the measured IR spectrum (Lambert-Beer law). In those systems, where a complete isomerization of one isomer was observed after irradiation, the amount of this isomer in the other spectra was directly calculated by relating it to this 100 % value. However, in most of the investigated systems no complete isomerization was obtained so that the extinction for 100% *E* or *Z* isomer had to be estimated using the following procedure: for each isomer one characteristic band with a strong intensity change after irradiation was chosen. From the change of the peak intensities for the highest and lowest amount of both isomers and the remaining intensities that were not extinguished by irradiation completely, the theoretical extinctions for 100 % *E* and 100 % *Z* isomer were estimated. Whenever possible, several such peaks were examined and a mean value was calculated. These mean values were used to determine the relative amounts of both isomers. A worked example is given on page 3 of the Supporting Information to illustrate this procedure.

**DSC/TGA.** DSC/TGA measurements were performed with a Mettler Toledo TGA/DSC 1 Star<sup>®</sup> (Al<sub>2</sub>O<sub>3</sub> crucible; Ar stream with 30 mL/min; heating rate 10 °C/min). Samples of approx. 2-6 mg were weighed out and handled under inert conditions (glovebox). Diagrams are visualized with Origin 8.5.0.<sup>[76]</sup>

## Acknowledgements

The authors gratefully acknowledge H. Emerich and C. Sternemann for their technical support and expertise at BM01B (ESRF/Grenoble) and BL9 (DELTA/Dortmund), S. Kremer for the elemental analyses, M. Pechtl for providing his IR spectrometer housed in a glovebox, and BASF SE for donating MOF-5. D.H. acknowledges the Fonds der Chemischen Industrie for a doctoral stipend.

**Keywords:** azobenzene • fluorinated derivatives • metal-organic frameworks • photochromism • solid state switching

- [1] H. Bouas-Laurent, H. Dürr, *Pure Appl. Chem.* **2001**, *73*, 639-665.
- [2] D. A. Parthenopoulos, P. M. Renetzepis, *Science* **1989**, *245*, 843-845.
- [3] Y. Hirshberg, *C. R. Hebd. Seances Acad. Sci.* **1950**, *116*, 903-904.
- [4] C. Li, Y. Zhang, J. Hu, J. Cheng, S. Liu, *Angew. Chem. Int. Ed.* **2010**, *49*, 5120-5124.
- [5] B. Liao, P. Long, B. He, S. Yi, B. Ou, S. Shen, J. Chen, *J. Mater. Chem. C* **2013**, *1*, 3716-3721.
- [6] J. Chen, F. Zeng, S. Wu, J. Zhao, Q. Chen, Z. Tong, *Chem. Commun.* **2008**, *13*, 5580-5582.
- [7] L. Zhu, M.-Q. Zhu, J. K. Hurst, A. D. Q. Li, *J. Am. Chem. Soc.* **2005**, *127*, 8968-8970.
- [8] D. Bléger, J. Dokić, M. V. Peters, L. Grubert, P. Saalfrank, S. Hecht, *J. Phys. Chem. B* **2011**, *115*, 9930-9940.
- [9] D.-J. Chung, Y. Ito, Y. Imanishi, *J. Appl. Polym. Sci.* **1994**, *51*, 2027-2033.

- [10] M. Moniruzzaman, C. J. Sabey, G. F. Fernando, *Polymer* **2007**, *48*, 255–263.
- [11] D. Bléger, T. Liebig, R. Thiermann, M. Maskos, J. P. Rabe, S. Hecht, *Angew. Chem. Int. Ed.* **2011**, *50*, 12559–12563.
- [12] M. Alemani, S. Selvanathan, F. Ample, M. V. Peters, K.-H. Rieder, F. Moresco, C. Joachim, S. Hecht, L. Grill, *J. Phys. Chem. C* **2008**, *112*, 10509–10514.
- [13] R. Klajn, *Chem. Soc. Rev.* **2014**, *43*, 148–184.
- [14] H. Tomioka, T. Itoh, *Chem. Commun.* **1991**, *7*, 532–533.
- [15] M. Irie, T. Fukaminato, K. Matsuda, S. Kobatake, *Chem. Rev.* **2014**, *114*, 12174–12277.
- [16] F. Marlow, K. Hoffmann, J. Caro, *Adv. Mater.* **1997**, *9*, 567–570.
- [17] K. Weh, M. Noack, K. Hoffmann, K.-P. Schröder, J. Caro, *Microporous Mesoporous Mater.* **2002**, *54*, 15–26.
- [18] K. Hoffmann, U. Resch-Genger, F. Marlow, *Microporous Mesoporous Mater.* **2000**, *41*, 99–106.
- [19] D.-H. Qu, Q.-C. Wang, Q.-W. Zhang, X. Ma, H. Tian, *Chem. Rev.* **2015**, *115*, 7543–7588.
- [20] D. Samanta, J. Gemen, Z. Chu, Y. Diskin-Posner, L. J. W. Shimon, R. Klajn, *Proc. Natl. Acad. Sci. USA* **2018**, *115*, 9379–9384.
- [21] S. Castellanos, F. Kapteijn, J. Gascon, *CrystEngComm* **2016**, *18*, 4006–4012.
- [22] L. Wang, Q. Li, *Chem. Soc. Rev.* **2018**, *47*, 1044–1097.
- [23] E. A. Dolgoplova, A. M. Rice, C. R. Martin, N. B. Shustova, *Chem. Soc. Rev.* **2018**, *47*, 4710–4728.
- [24] G. Férey, *Chem. Soc. Rev.* **2008**, *37*, 191–214.
- [25] C. Janiak, *Dalton Trans.* **2003**, 2781–2804.
- [26] A. Schaate, S. Dühnen, G. Platz, S. Lilienthal, A. M. Schneider, P. Behrens, *Eur. J. Inorg. Chem.* **2012**, 790–796.
- [27] C. C. Epley, K. L. Roth, S. Lin, S. R. Ahrenholtz, T. Z. Grove, A. J. Morris, *Dalton Trans.* **2017**, *46*, 4917–4922.
- [28] J. Zhang, L. Wang, N. Li, J. Liu, W. Zhang, Z. Zhang, N. Zhou, X. Zhu, *CrystEngComm* **2014**, *16*, 6547–6551.
- [29] A. Modrow, D. Zargarani, R. Herges, N. Stock, *Dalton Trans.* **2011**, *40*, 4217–4222.
- [30] J. Park, D. Yuan, K. T. Pham, J.-R. Li, A. Yakovenko, H.-C. Zhou, *J. Am. Chem. Soc.* **2012**, *134*, 99–102.
- [31] X. Yu, Z. Wang, M. Buchholz, N. Füllgrabe, S. Grosjean, F. Bebensee, S. Bräse, C. Wöll, L. Heinke, *Phys. Chem. Chem. Phys.* **2015**, *17*, 22721–22725.
- [32] L. Heinke, M. Cakici, M. Dommaschk, S. Grosjean, R. Herges, S. Bräse, C. Wöll, *ACS Nano* **2014**, *8*, 1463–1467.
- [33] L. Heinke, *J. Phys. D. Appl. Phys.* **2017**, *50*, 193004.
- [34] A. B. Kanj, K. Müller, L. Heinke, *Macromol. Rapid Commun.* **2018**, *39*, 1700239 (14 pages).
- [35] S. Castellanos, A. Goulet-Hanssens, F. Zhao, A. Dikhtiarenko, A. Pustovarenko, S. Hecht, J. Gascon, F. Kapteijn, D. Bléger, *Chem. Eur. J.* **2016**, *22*, 746–752.
- [36] K. Müller, A. Knebel, F. Zhao, D. Bléger, J. Caro, L. Heinke, *Chem. Eur. J.* **2017**, *23*, 5434–5438.
- [37] D. E. Williams, C. R. Martin, E. A. Dolgoplova, A. Swifton, D. C. Godfrey, O. A. Ejegbavwo, P. J. Pellechia, M. D. Smith, N. B. Shustova, *J. Am. Chem. Soc.* **2018**, *140*, 7611–7622.
- [38] H. A. Schwartz, U. Ruschewitz, L. Heinke, *Photochem. Photobiol. Sci.* **2018**, *17*, 864–873.
- [39] N. Yanai, T. Uemura, M. Inoue, R. Matsuda, T. Fukushima, M. Tsujimoto, S. Isoda, S. Kitagawa, *J. Am. Chem. Soc.* **2012**, *134*, 4501–4504.
- [40] D. Hermann, H. Emerich, R. Lepski, D. Schaniel, U. Ruschewitz, *Inorg. Chem.* **2013**, *52*, 2744–2749.
- [41] F. Zhang, X. Zou, W. Feng, X. Zhao, X. Jing, F. Sun, H. Ren, G. Zhu, *J. Mater. Chem.* **2012**, *22*, 25019–25026.
- [42] H. A. Schwartz, S. Olthof, D. Schaniel, K. Meerholz, U. Ruschewitz, *Inorg. Chem.* **2017**, *56*, 13100–13110.
- [43] I. M. Walton, J. M. Cox, J. A. Coppin, C. M. Linderman, D. G. Patel, J. B. Benedict, *Chem. Commun.* **2013**, *49*, 8012–8014.
- [44] K. Ohara, Y. Inokuma, M. Fujita, *Angew. Chem. Int. Ed.* **2010**, *49*, 5507–5509.
- [45] Y. Zheng, H. Sato, P. Wu, H. J. Jeon, R. Matsuda, S. Kitagawa, *Nat. Commun.* **2017**, *8*, Article number: 100.
- [46] M. Kojima, M. Nakajoh, S. Nebashi, N. Kurita, *Res. Chem. Intermed.* **2004**, *30*, 181–190.
- [47] H. A. Wegner, *Angew. Chem. Int. Ed.* **2012**, *51*, 4787–4788.
- [48] D. Bléger, J. Schwarz, A. M. Brouwer, S. Hecht, *J. Am. Chem. Soc.* **2012**, *134*, 20597–20600.
- [49] D. Hermann, H. A. Schwartz, U. Ruschewitz, *ChemistrySelect* **2017**, *2*, 11846–11852.
- [50] K. Müller, J. Wadhwa, J. S. Malhi, L. Schöttner, A. Welle, H. Schwartz, D. Hermann, U. Ruschewitz, L. Heinke, *Chem. Commun.* **2017**, *53*, 8070–8073.
- [51] H. M. D. Bandara, S. C. Burdette, *Chem. Soc. Rev.* **2012**, *41*, 1809–1825.
- [52] C. Knie, M. Utecht, F. Zhao, H. Kulla, S. Kovalenko, A. M. Brouwer, P. Saalfrank, S. Hecht, D. Bléger, *Chem. Eur. J.* **2014**, *20*, 16492–16501.
- [53] T. Loiseau, C. Serre, C. Huguenard, G. Fink, F. Taulelle, M. Henry, T. Bataille, G. Férey, *Chem. Eur. J.* **2004**, *10*, 1373–1382.
- [54] H. Li, M. Eddaoudi, M. O’Keeffe, O. M. Yaghi, *Nature* **1999**, *402*, 276–279.
- [55] R. S. Rowland, R. Taylor, *J. Phys. Chem.* **1996**, *100*, 7384–7391.
- [56] J. Hernández-Trujillo, A. Vela, *J. Phys. Chem.* **1996**, *100*, 6524–6530.
- [57] C. A. Hunter, K. R. Lawson, J. Perkins, C. J. Urch, *J. Chem. Soc., Perkin Trans.* **2001**, *2*, 651–669.
- [58] C. Volkringer, T. Loiseau, N. Guillou, G. Férey, E. Elkaim, A. Vimont, *Dalton Trans.* **2009**, 2241–2249.
- [59] D. Das, H. Agarkar, *ACS Omega* **2018**, *3*, 7630–7638.
- [60] S. Kobatake, S. Takami, H. Muto, T. Ishikawa, M. Irie, *Nature* **2007**, *446*, 778–781.
- [61] J. Liu, F. Zhang, X. Zou, S. Zhou, L. Li, F. Sun, S. Qiu, *Eur. J. Inorg. Chem.* **2012**, 5784–5790.
- [62] C. Volkringer, M. Meddouri, T. Loiseau, N. Guillou, J. Marrot, G. Férey, M. Haouas, F. Taulelle, N. Audebrand, M. Latroche, *Inorg. Chem.* **2008**, *47*, 11892–11901.
- [63] J. M. Birchall, R. N. Haszeldine, J. E. G. Kemp, *J. Chem. Soc. C* **1970**, 449–455.
- [64] S. Hettel, PhD thesis, University of Cologne (Germany), **2009**.
- [65] W. Van Beek, O. V. Safonova, G. Wiker, H. Emerich, *Phase Transitions* **2011**, *84*, 726–732.
- [66] C. Krywka, C. Sternemann, M. Paulus, N. Javid, R. Winter, A. Al-Sawalmih, S. Yi, D. Raabe, M. Tolan, *J. Synchrotron Radiat.* **2007**, *14*, 244–251.
- [67] *STOE Win XPOW 1.07*, STOE & Cie GmbH, Darmstadt, Germany, **2000**.
- [68] V. Petříček, M. Dušek, L. Palatinus, Jana2006: The Crystallographic Computing System; Institute of Physics, Praha, Czech Republic, **2006**.
- [69] T. Williams, C. Kelley, R. Lang, *Gnuplot 4.6*, **2012**.
- [70] M. Vougo-Zanda, J. Huang, E. Anokhina, X. Wang, A. J. Jacobson, *Inorg. Chem.* **2008**, *47*, 11535–11542.
- [71] K. Chinnakali, H.-K. Fun, *Acta Crystallogr.* **1993**, *C49*, 615–616.
- [72] V. Favre-Nicolin, R. Černý, *J. Appl. Crystallogr.* **2002**, *35*, 734–743.
- [73] a) A. C. Larson, R. B. v. Dreele, General Structure Analysis System (GSAS). *Los Alamos National Laboratory Report LAUR* **2004**, 86–748; b) B. H. Toby, *J. Appl. Crystallogr.* **2001**, *34*, 210–213.
- [74] K. Brandenburg, *Diamond 3.2i*, Crystal Impact GbR, Bonn, Germany, **2012**.
- [75] ACD/NMR Processor Academic Edition 12.01, Advanced Chemistry Development, Inc., **2010**.
- [76] *OriginPro* Version 8.5.0G, OriginLab Corporation, Northhampton USA, **1991–2010**.

**Table 1.** Selected optical properties of azobenzene and some fluorinated derivatives.

	absorption maxima	photoisomerization	thermal half-life of Z isomer	Reference(s)
<i>E</i> -AZB	320 nm ( $\pi, \pi^*$ ) 450 nm ( $n, \pi^*$ )	46-53 % <i>Z</i> -AZB ( $\lambda = 366$ nm, cyclohexane)		[46,51,52]
<i>Z</i> -AZB	250, 270 nm ( $\pi, \pi^*$ ) 450 nm ( $n, \pi^*$ )		$t_{1/2} = 2$ days (room temperature) $t_{1/2} = 4$ h (60 °C, acetonitrile)	
<i>E</i> - <i>t</i> F-AZB	305 nm ( $\pi, \pi^*$ ) 458 nm ( $n, \pi^*$ )	84 % <i>Z</i> - <i>t</i> F-AZB ( $\lambda = 313$ nm, acetonitrile) 91 % <i>Z</i> - <i>t</i> F-AZB ( $\lambda > 450$ nm, acetonitrile)		[48,52]
<i>Z</i> - <i>t</i> F-AZB	414 nm ( $n, \pi^*$ )	86 % <i>E</i> - <i>t</i> F-AZB ( $\lambda = 410$ nm, acetonitrile)	$t_{1/2} = 700$ days (25 °C) $t_{1/2} = 92$ h (60 °C)	
<i>E</i> - <i>o</i> F-AZB	303 nm ( $\pi, \pi^*$ ) 456 nm ( $n, \pi^*$ )	92 % <i>Z</i> - <i>o</i> F-AZB ( $\lambda > 500$ nm, acetonitrile)		[52]
<i>Z</i> - <i>o</i> F-AZB	~240 nm ( $\pi, \pi^*$ ) 413 nm ( $n, \pi^*$ )	92 % <i>E</i> - <i>o</i> F-AZB ( $\lambda = 410$ nm, acetonitrile)	$t_{1/2} = 27$ h (60 °C)	
<i>E</i> - <i>p</i> F-AZB	310 nm ( $\pi, \pi^*$ ) 453 nm ( $n, \pi^*$ )	91 % <i>Z</i> - <i>p</i> F-AZB ( $\lambda > 500$ nm, acetonitrile)		[52]
<i>Z</i> - <i>p</i> F-AZB	473 nm ( $n, \pi^*$ )	90 % <i>E</i> - <i>p</i> F-AZB ( $\lambda = 410$ nm, acetonitrile)	not determined	

**Table 3.** Maximum amounts of *E* and *Z* isomers for the investigated *F*-AZB@MOF systems, achieved by illumination with 405 and 532 nm, respectively.

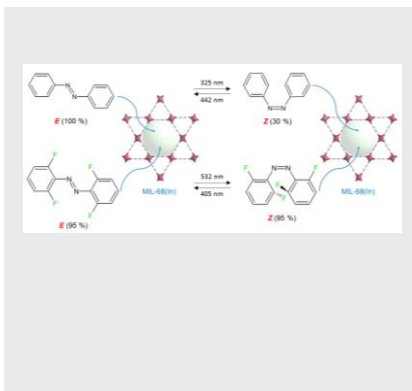
	AZB <sup>[40]</sup>	<i>t</i> F-AZB	<i>o</i> F-AZB	<i>p</i> F-AZB
	max. <i>E</i> / max. <i>Z</i> , [initial state]	max. <i>E</i> / max. <i>Z</i> , [initial state]	max. <i>E</i> / max. <i>Z</i> , [initial state]	max. <i>E</i> / max. <i>Z</i> , [initial state]
MOF-5	100 % / 25 % [100 % <i>E</i> ]	93 % / 82 % [52 % <i>E</i> ]	n.d. [62–88 % <i>E</i> ]	100 % / 50 % [80 % <i>E</i> ]
MIL-53(Al)	100 % / 0 % [100 % <i>E</i> ]	90 % / 100 % [37 % <i>E</i> ]	100 % / 56 % [99 % <i>E</i> ]	100 % / little <i>Z</i> [100 % <i>E</i> ]
MIL-53(Ga)	100 % / n.d. [100 % <i>E</i> ]	90 % / 94 % [37 % <i>E</i> ]	n.d. [little <i>Z</i> ]	100 % / n.d. [100 % <i>E</i> ]
MIL-68(Ga)	100 % / 27 % [100 % <i>E</i> ]	96 % / 93 % [45 % <i>E</i> ]	n.d. [62–88 % <i>E</i> ]	100 % / 40 % [87 % <i>E</i> ]
MIL-68(In)	100 % / 30 % [100 % <i>E</i> ]	95 % / 95 % [51 % <i>E</i> ]	88 % / 90 % [62 % <i>E</i> ]	100 % / 79 % [55 % <i>E</i> ]

n.d.: not determined

## Entry for the Table of Contents

## FULL PAPER

Azobenzenes with different degrees of fluorination were embedded into the pores of the metal-organic frameworks MOF-5, MIL-53(Al), MIL-53(Ga), MIL-68(Ga), MIL-68(In) and thoroughly characterized thereafter. All synthesized *F*-AZB@MOF systems can be switched with visible light and some of them show almost quantitative (> 95 %) photoisomerization between its *E* and *Z* forms with no significant fatigue after repeated switching cycles.



Daniela Hermann, Heidi A. Schwartz, Melanie Werker, Dominik Schaniel, Uwe Ruschewitz\*

Page No. – Page No.

**Metal-Organic Frameworks as Hosts for Fluorinated Azobenzenes: A Path Towards Quantitative Photoswitching with Visible Light**